Insertion, Adduct Formation, and Elimination of Alkenes in Gas-Phase Reactions of Bis(η^5-cyclopentadienyl)methylzirconium(1+) with Nitriles

Charles S. Christ, Jr., John R. Eyler, and David E. Richardson*,†

Contribution from the Department of Chemistry, University of Florida, Gainesville, Florida 32611. *Received May 4, 1989. Revised Manuscript Received December 11, 1989*

Abstract: The gas-phase reactions of $Cp_2ZrCH_3^+$, (**1**, Cp = cyclopentadienyl) with a number of alkyl nitriles and benzonitrile have been studied by using Fourier transform ion cyclotron resonance mass spectrometry. The formation of adducts occurs readily for all nitriles investigated, and the rate constants for adduct formation in the reaction of **1** with acetonitrile were determined. The rate constants range from $0.05k_c$–$0.15k_c$ as buffer gas pressures are increased from 0 to $\sim 1.5 \times 10^{-6}$ Torr, where k_c is the estimated ion/molecule collision rate (2.2×10^{-9} cm^3 s^{-1}). Insertion of nitriles is proposed to yield azomethine complexes, and in several cases the reverse reaction, deinsertion, produces Cp_2ZrR^+ and $N{\equiv}CCH_3$, where R is the alkyl or phenyl portion of the nitrile substrate. Comparisons of reactivity of the gas-phase ion **1** to solution chemistry are considered, since both adduct formation and insertion have been observed for d^0f^n complexes in solution. Reactions of **1** with *n*-alkyl nitriles having alkyl groups larger than methyl result in elimination of alkenes producing $Cp_2ZrN{=}C(H)(CH_3)^+$, presumably by a mechanism involving deinsertion. Formation of Zr–allyl complexes is also observed for reaction of **1** with $R{-}C{\equiv}N$ (R = propyl, butyl). Lower limits for relative Cp_2Zr^+–R bond disruption enthalpies are derived where possible and indicate that relative bond disruption enthalpies for $Cp_2Zr{-}R^+$ complexes are similar to those reported for related neutral complexes in solution. The reactivity of **1** with nitriles is comparable to reactivity of analogous neutral and cationic d^0f^n metal complexes, but additional reaction pathways are observed in the gas phase.

Electrophilic organometallic, lanthanide, actinide, and early transition-metal alkyls and hydrides have recently been reported to coordinate and insert nitriles.[1-8] In some instances, it is possible to isolate simple coordination complexes,[9] and, in other cases, insertion takes place rapidly and an intermediate nitrile adduct is not observed.[3,10] Certain azomethine insertion products react with a second equivalent of nitrile yielding an isolable metallo-heterocycle.[6,10] Nitrile insertion is also known for aluminum alkyls and hydrides[11,12] and generally occurs when the nitrile adducts are heated.[13] Reactions of the higher alkyls of aluminum indicate that oxidation of the alkyl ligands to alkenes competes with insertion.

We have a continuing interest in developing relevant comparisons of the reactivities of organometallic complex ions in the gas phase and solution.[14] The reactivity of the gas-phase electrophilic cation $Cp_2ZrCH_3^+$ (**1**, Cp = cyclopentadienyl) with unsaturated hydrocarbons and dihydrogen was described in earlier publications.[14a,b] These studies demonstrated that solvent plays a substantial role in directing the reaction pathways for this organometallic ion with certain substrates. For example, dehydrogenation rather than β-hydride shift/alkene elimination is the major decomposition pathway for gas-phase alkyl complexes formed by insertion of alkenes. In other ways, the gas-phase reactivity closely parallels the solution chemistry of Cp_2ZrR^+ and other isoelectronic complexes. For example, C–H activation of substrates becomes increasingly favorable for increasing s character at the C (i.e., $sp > sp^2 > sp^3$). Here we report that many of the same mechanistic pathways reported for the reactions of condensed-phase d^0f^n complexes with nitriles are also found for $Cp_2ZrCH_3^+$(g). In addition, the formation of nitrile adducts has been found to be unexpectedly rapid, and we have investigated the mechanism by kinetic studies of adduct formation.

Gas-phase reactions in this work are studied by using Fourier transform ion cyclotron resonance mass spectrometry (FTICR).[15] The absence of direct structural probes in the present configuration of the FTICR is compensated somewhat by the nature of $Cp_2ZrCH_3^+$. This zirconium(IV) alkyl cation is formally d^0 and therefore is not expected to undergo oxidative addition, which limits the number of reasonable structures proposed for product ions and mechanistic sequences available to describe the various reactions observed. Furthermore, a substantial amount of insight into possible reaction pathways in the gas-phase ion chemistry of **1** can be obtained by reference to condensed-phase results. The present work is a report of the reactions of $Cp_2ZrCH_3^+$(g) with several alkyl nitriles and benzonitrile. Attempts are made to compare gas-phase and solution reactivity whenever possible, and some thermodynamic data are also derived for relative Zr–R bond disruption enthalpies of these cationic complexes.

Results

We applied FTICR mass spectrometry to study the reactions of **1** with several *n*-alkyl nitriles, *t*BuCN, and benzonitrile. Reactions were monitored as a function of time until no net change

† A. P. Sloan Foundation Research Fellow, 1988–1990.

(1) (a) Bochmann, M.; Wilson, L. M.; Hursthouse, M. B.; Motevalli, M. *Organometallics* **1988**, *7*, 1148. (b) Bochmann, M.; Wilson, L. M. *Organometallics* **1987**, *6*, 2556. (c) Bochmann, M.; Wilson, L. M. *J. Chem. Soc., Chem. Commun.* **1986**, 1610.
(2) Simpson, S. J.; Anderson, R. A. *J. Am. Chem. Soc.* **1981**, *103*, 4063.
(3) den Haan, K. H.; Wielstra, G. H.; Meetsma, A.; Teuben, J. H. *Organometallics* **1987**, *6*, 1513.
(4) Dormond, A.; Aaliti, A.; El Bonadili, A.; Miose, C. *J. Organomet. Chem.* **1987**, *329*, 187.
(5) Cramer, R. E.; Panchanatheswaran, K.; Gilje, J. W. *J. Am. Chem. Soc.* **1984**, *106*, 1853.
(6) Richeson, D. S.; Mitchell, J. F.; Theopold, K. H. *J. Am. Chem. Soc.* **1987**, *109*, 5868.
(7) Sternal, R. S.; Sabat, M.; Marks, T. J. *J. Am. Chem. Soc.* **1987**, *109*, 7920.
(8) Churchill, M. R.; Wasserman, H. J.; Belmont, P. A.; Schrock, R. R. *Organometallics* **1982**, *1*, 559.
(9) Jordan, R. F.; Bajgur, C. S.; Dasher, W. E. *Organometallics* **1987**, *6*, 1041.
(10) Bercaw, J. E.; Davies, D. L.; Wolczanski, P. T. *Organometallics* **1986**, *5*, 443.
(11) (a) Lloyd, J. E.; Wade, K. *J. Chem. Soc.* **1965**, 2662. (b) Jennings, J. R.; Lloyd, J. E.; Wade, K. *J. Chem. Soc.* **1965**, 5083.
(12) Lardicci, L.; Giacomelli, G. P. *J. Organomet. Chem.* **1971**, *33*, 293.
(13) (a) Bagnell, L.; Jeffery, E. A.; Meisters, A.; Mole, T. *Aust. J. Chem.* **1974**, *27*, 2577. (b) Mole, T.; Jeffery, E. A. *Organoaluminum Compounds*; Elsevier: Amsterdam, 1972; Chapter 12.
(14) (a) Christ, C. S.; Eyler, J. R.; Richardson, D. E. *J. Am. Chem. Soc.* **1988**, *110*, 4038. (b) Christ, C. S.; Eyler, J. R.; Richardson, D. E. *J. Am. Chem. Soc.* **1990**, *112*, 596. (c) Richardson, D. E.; Christ, C. S.; Sharpe, P.; Eyler, J. R. *J. Am. Chem. Soc.* **1987**, *109*, 3894. (d) Richardson, D. E.; Christ, C. S.; Sharpe, P.; Eyler, J. R. *Organometallics* **1987**, *6*, 1819.
(15) (a) Marshall, A. G. *Acc. Chem. Res.* **1985**, *18*, 316. (b) Wanczek, K. P. *Int. J. Mass Spec. Ion Proc.* **1984**, *60*, 11. (c) Gross, M. L.; Rempel, D. L. *Science (Washington, D.C.)* **1984**, *226*, 261.

0002-7863/90/1512-4778$02.50/0

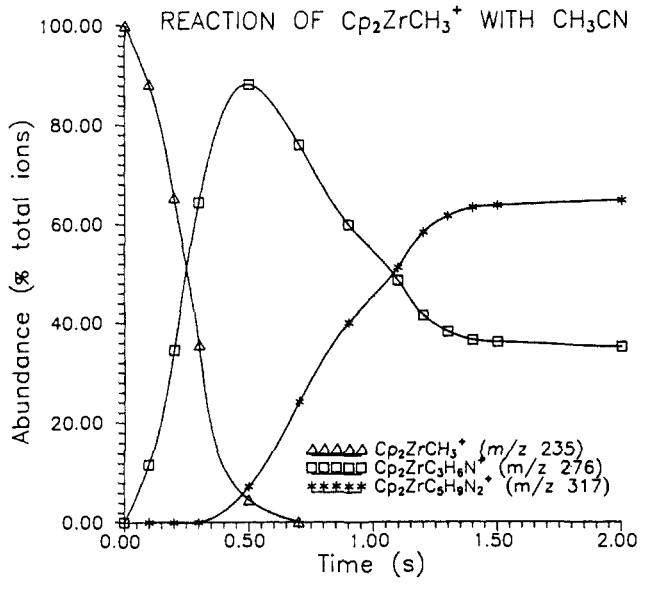

Figure 1. Ion abundance vs time for the reaction of **1** with CH_3CN. Data are normalized to the total ion abundance and fit with a cubic spline.

in the relative abundance of the product ions occurred.

Zirconium product ions of the form $Cp_2ZrC_xH_yN_z^+$ yield seven observed principal isotopic species. For clarity, the product ions are reported as a single (m/z) value corresponding to isotopic species containing the most abundant ^{90}Zr isotope. In this section product ions are indicated by an empirical formula $Cp_2ZrC_xH_yN_z^+$, and no structure is implied other than the Cp_2Zr unit. The eliminated neutral is taken to be the most stable species possible with the correct molecular formula. Detailed structures of the Zr product ions will be presented in the Discussion section.

Collision-induced dissociation (CID)[16-18] of **1** shows only the loss of $^{\bullet}CH_3$, strongly implying a metal methyl structure. Reaction of $Cp_2ZrCD_3^+$ with CD_3CN and CID of the resulting products shows an absence of H/D scrambling even in the high-energy CID experiment, indicating that involvement of the Cp ligand hydrogens is insignificant in these transformations.

Reaction of $Cp_2ZrCH_3^+$ with CH_3CN. The interaction of **1** with CH_3CN results in two sequential reactions producing $Cp_2ZrC_3H_6N^+$ (m/z 276) and $Cp_2ZrC_5H_9N_2^+$ (m/z 317) (eqs 1 and 2). However, the reaction represented in eq 2 does not

$$\underset{(m/z\ 235)}{Cp_2ZrCH_3^+} + CH_3CN \rightarrow \underset{(m/z\ 276)}{Cp_2ZrC_3H_6N^+} \quad (1)$$

$$\underset{(m/z\ 276)}{Cp_2ZrC_3H_6N^+} + CH_3CN \rightarrow \underset{(m/z\ 317)}{Cp_2ZrC_5H_9N_2^+} \quad (2)$$

proceed to completion (i.e., not all of m/z 276 ions are converted to m/z 317, Figure 1). The final ratio of m/z 276:m/z 317 is approximately 0.6 ± 0.1 and shows little variation as the internal energy of **1** is increased by raising the EI beam voltage from 11 to 20 eV. The final ratio is also invariant in the presence of argon or cyclohexane buffer gas up to 5×10^{-6} Torr.

The second-order rate coefficient for formation of m/z 276 is only weakly dependent on buffer gas pressure at various CH_3CN pressures (5×10^{-7}, 1×10^{-6} and 2×10^{-6} Torr) when Ar and Kr are used as buffers. The second-order rate coefficient is $1.2 \pm 0.3 \times 10^{-10}$ (Kr pressure = 0–2×10^{-6} Torr), $1.9 \pm 0.9 \times 10^{-10}$ (Ar pressure = 3×10^{-6} Torr), and $3.3 \pm 3.6 \times 10^{-10}$ cm^3 s^{-1} (Ar pressure = 1.5×10^{-5} Torr). The ADO collisional rate coefficient[19] for formation of m/z 276 is 2.2×10^{-9} cm^3 s^{-1}, significantly higher than the measured rate coefficients.

Experiments on the effect of increasing nitrile pressure indicate that the reaction shown in eq 2 is not an equilibrium. Ejection of m/z 276 after the ion population has become constant shows no back reaction to reform m/z 276; likewise, ejection of m/z 317 proves no subsequent forward reaction occurs. However, unreacted m/z 276 can be converted to m/z 317 in the following manner. Low-energy RF irradiation of m/z 276 causes an increase in the translational energy of the ions without inducing collisional fragmentation. The effect of this translational excitation followed by collisions with buffer gas and reaction with CH_3CN is measured as an increase in the abundance of m/z 317; i.e., a portion of the unreactive $Cp_2ZrC_3H_6N^+$ (m/z 276) is converted to $Cp_2ZrC_5H_9N_2^+$ (m/z 317) by increasing the total energy of m/z 276 and allowing time for reaction with CH_3CN.

In conventional FTICR CID experiments on m/z 317, the formation of m/z 276 is observed at lower energies (eq 3), and as the CID energy is increased m/z 235 and m/z 220 are also detected (eqs 4 and 5).

$$\underset{(m/z\ 317)}{Cp_2ZrC_5H_9N_2^+} \xrightarrow{CID} \begin{cases} \underset{(m/z\ 276)}{Cp_2ZrC_3H_6N^+} + CH_3CN & (3) \\ \underset{(m/z\ 235)}{Cp_2ZrCH_3^+} + 2CH_3CN & (4) \\ \underset{(m/z\ 220)}{Cp_2Zr^{\bullet+}} + 2CH_3CN + {}^{\bullet}CH_3 & (5) \end{cases}$$

CID of m/z 276 before the final ratio is established is consistent with CID of m/z 317 (eqs 6 and 7). Furthermore, after the final ratio of m/z 276:m/z 317 is attained, the same product fragments are observed for CID of m/z 276.

$$\underset{(m/z\ 276)}{Cp_2ZrC_3H_6N^+} \xrightarrow{CID} \begin{cases} \underset{(m/z\ 235)}{Cp_2ZrCH_3^+} + CH_3CN & (6) \\ \underset{(m/z\ 220)}{Cp_2Zr^{\bullet+}} + CH_3CN + {}^{\bullet}CH_3 & (7) \end{cases}$$

Reactions of **1** with CD_3CN are exactly analogous to those for CH_3CN; however, this substrate allows the detection of a product previously indistinguishable from the reactant cation **1**. $Cp_2ZrCD_3^+$ (m/z 238) is formed in the early stages of the reaction (eq 8). Complete conversion of $Cp_2ZrCH_3^+$ to $Cp_2ZrCD_3^+$ does not occur before addition of CD_3CN forms m/z 279 (eq 9). Any $Cp_2ZrCD_3^+$ formed also reacts to produce $Cp_2ZrC_3D_6N^+$ (m/z 282). Detectable production of $Cp_2ZrCD_3^+$ (eq 8) can be completely suppressed by using a low pressure of CD_3CN (1×10^{-7} Torr) and a high pressure of cyclohexane buffer gas (5×10^{-6} Torr).

$$\underset{(m/z\ 235)}{Cp_2ZrCH_3^+} + CD_3CN \rightarrow \underset{(m/z\ 238)}{Cp_2ZrCD_3^+} + CH_3CN \quad (8)$$

$$\underset{(m/z\ 235)}{Cp_2ZrCH_3^+} + CD_3CN \rightarrow \underset{(m/z\ 279)}{Cp_2ZrC_3H_3D_3N^+} \quad (9)$$

Reaction of $Cp_2ZrCH_3^+$ with *t*BuCN. Reaction of **1** with *t*BuCN ($(CH_3)_3CCN$) is similar to reaction with CH_3CN in that two sequential additions of nitrile occur to produce $Cp_2ZrC_6H_{12}N^+$ (m/z 318) and $Cp_2ZrC_{11}H_{21}N_2^+$ (m/z 401) (eqs 10 and 11). In

$$\underset{(m/z\ 235)}{Cp_2ZrCH_3^+} + t\text{BuCN} \rightarrow \underset{(m/z\ 318)}{Cp_2ZrC_6H_{12}N^+} \quad (10)$$

$$\underset{(m/z\ 318)}{Cp_2ZrC_6H_{12}N^+} + t\text{BuCN} \rightarrow \underset{(m/z\ 401)}{Cp_2ZrC_{11}H_{21}N_2^+} \quad (11)$$

analogy to the CH_3CN system, the reaction depicted in eq 11 does not proceed to completion. The final ratio m/z 318:m/z 401 is 5.5 ± 0.1. After the system attains the constant final ratio of m/z 318:m/z 401, low power RF irradiation of m/z 318 is effective in promoting the conversion of m/z 318 to m/z 401 in a manner

(16) (a) Jacobson, D. B.; Freiser, B. S. *J. Am. Chem. Soc.* **1983**, *105*, 736. (b) Cody, R. B.; Freiser, B. S. *Int. J. Mass Spectrom. Ion Phys.* **1982**, *41*, 199.
(17) Freas, R. B.; Ridge, D. P. *J. Am. Chem. Soc.* **1980**, *102*, 7129.
(18) Cooks, R. G. *Collision Spectrosc.* **1978**, 357.
(19) Su, T.; Bowers, M. T. *J. Chem. Phys.* **1973**, *58*, 3027.

Scheme I

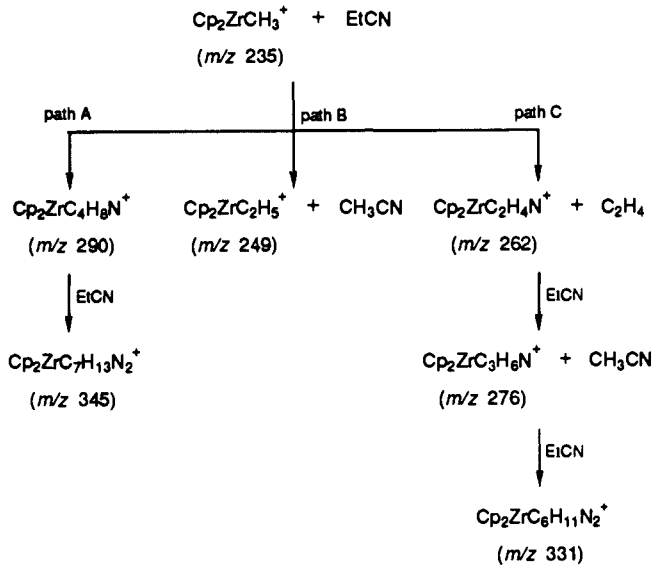

exactly analogous to the experiments involving m/z 276 and CH_3CN described above.

The results of CID experiments on m/z 401 and m/z 318 resemble those for CID of the products formed in the reaction of **1** with CH_3CN. Apparent loss of *t*BuCN occurs from both m/z 318 and m/z 401 (eqs 12 and 13). Infrared multiphoton dissociation (IRMPD)[20,21] of $Cp_2ZrC_6H_{12}N^+$ (m/z 318) using a continuous wave CO_2 laser (1090 cm^{-1}) is consistent with results of CID experiments, producing the $Cp_2ZrCH_3^+$ fragment ion.

$$\underset{(m/z\ 401)}{Cp_2ZrC_{11}H_{21}N_2^+} \xrightarrow{CID} \underset{(m/z\ 318)}{Cp_2ZrC_6H_{12}N^+} + t\text{BuCN} \quad (12)$$

$$\underset{(m/z\ 318)}{Cp_2ZrC_6H_{12}N^+} \xrightarrow{CID} \underset{(m/z\ 235)}{Cp_2ZrCH_3^+} + t\text{BuCN} \quad (13)$$

Reaction of $Cp_2ZrCH_3^+$ with PhCN. In the reaction of **1** with cyanobenzene nearly 90% of **1** is converted to Cp_2ZrPh^+ (m/z 297) (eq 14). Cp_2ZrPh^+ reacts with PhCN to produce

$$\underset{(m/z\ 235)}{Cp_2ZrCH_3^+} + PhCN \rightarrow \underset{(m/z\ 297)}{Cp_2ZrPh^+} + CH_3CN \quad (14)$$

$Cp_2ZrCPh_2N^+$ (m/z 400) (eq 15). Addition of PhCN to $Cp_2ZrCPh_2N^+$ yields $Cp_2ZrC_2Ph_3N_2^+$ (m/z 503) (eq 16), but

$$\underset{(m/z\ 297)}{Cp_2ZrPh^+} + PhCN \rightarrow \underset{(m/z\ 400)}{Cp_2ZrCPh_2N^+} \quad (15)$$

$$\underset{(m/z\ 400)}{Cp_2ZrCPh_2N^+} + PhCN \rightarrow \underset{(m/z\ 503)}{Cp_2ZrC_2Ph_3N_2^+} \quad (16)$$

again in analogy to results above for acetonitrile and *tert*-butyl nitrile this addition does not convert all m/z 400 to m/z 503. The final ratio, m/z 400:m/z 503, is 0.3 ± 0.1. $Cp_2ZrCH_3^+$ also adds one and two PhCN units to produce $Cp_2ZrC_2H_3PhN^+$ (m/z 318) (eq 17) and $Cp_2ZrC_3H_3Ph_2N_2^+$ (m/z 441) (eq 18), respectively. However, a reliable measurement of the final ratio m/z 338:m/z 441 is unattainable due to the low intensity of these product ions.

$$\underset{(m/z\ 235)}{Cp_2ZrCH_3^+} + PhCN \rightarrow \underset{(m/z\ 318)}{Cp_2ZrC_2PhH_3N^+} \quad (17)$$

$$\underset{(m/z\ 318)}{Cp_2ZrC_2PhH_3N^+} + PhCN \rightarrow \underset{(m/z\ 441)}{Cp_2ZrC_3Ph_2H_3N_2^+} \quad (18)$$

CID of $Cp_2ZrC_2Ph_3N_2^+$ (m/z 503) yields $Cp_2ZrCPh_2N^+$ (m/z 400), which is the reverse of eq 16. Increasing CID energy causes the loss of two PhCN units and formation of Cp_2ZrPh^+. However, $Cp_2Zr^{\bullet+}$ is not observed even at high CID energies.

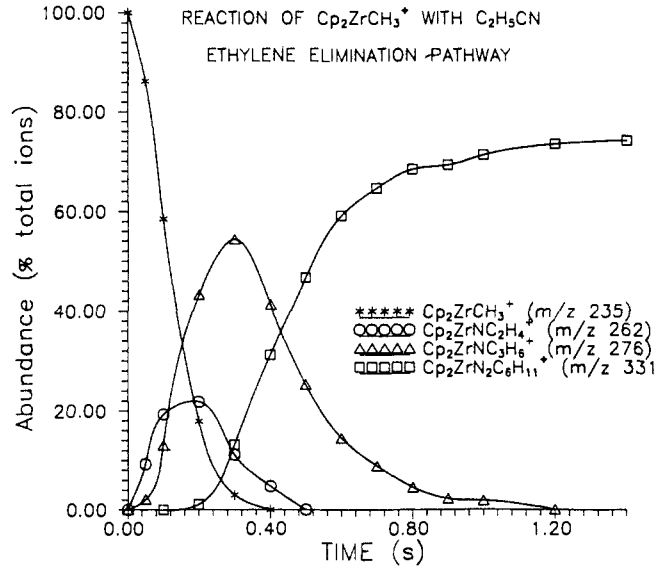

Figure 2. Ion abundance vs time for the major reaction pathway in the reaction of **1** with EtCN. For clarity all product ions are not represented. Data are normalized to the total ion abundance and fit with a cubic spline.

Reaction of $Cp_2ZrCH_3^+$ with EtCN. The reaction of **1** with EtCN gives several products and is summarized in Scheme I. Approximately 80% of the total product ion intensity is accounted for in a single reaction pathway involving the production of $Cp_2ZrC_6H_{11}N_2^+$ (m/z 331) (path C in Scheme I and Figure 2).

CID experiments on the m/z 331 product ion show fragmentation to form $Cp_2ZrC_3H_6N^+$ (m/z 276) (eq 19). As CID energy

$$\underset{(m/z\ 331)}{Cp_2ZrC_6H_{11}N_2^+} \xrightarrow{CID} \underset{(m/z\ 276)}{Cp_2ZrC_3H_6N^+} + \text{EtCN} \quad (19)$$

is increased Cp_2ZrH^+ (m/z 221) is observed in a 9-fold excess over $Cp_2ZrC_2H_5^+$ (m/z 249). IRMPD of m/z 331 is in agreement with the CID results represented in eq 19, and no other fragments are detected. CID of $Cp_2ZrC_3H_6N^+$ (m/z 276) produces Cp_2ZrH^+ in higher abundance than $Cp_2ZrC_2H_5^+$ resulting in CID spectra similar to that recorded for high-energy CID of $Cp_2ZrC_6H_{11}N_2^+$. Finally, Cp_2ZrH^+ is the only fragment ion observed, other than Cp_2Zr^+, in the CID of $Cp_2ZrC_2H_4N^+$ (m/z 262) (eq 20).

$$\underset{(m/z\ 262)}{Cp_2ZrC_2H_4N^+} \xrightarrow{CID} \underset{(m/z\ 221)}{Cp_2ZrH^+} + \text{EtCN} \quad (20)$$

Approximately 18% of the product ions are formed via an addition pathway similar to that observed for CH_3CN and *t*BuCN (path A in Scheme I and Figure 3). The final ratio of m/z 290:m/z 345 is 0.8 ± 0.1. CID of product ions formed in the addition pathway is precluded by their low intensity.

Reaction of $Cp_2ZrCH_3^+$ with *n*PrCN and *n*BuCN. The reactions of $Cp_2ZrCH_3^+$ with *n*PrCN ($CH_3CH_2CH_2CN$) and *n*BuCN ($CH_3CH_2CH_2CH_2CN$) are summarized in Scheme II. The general reactivity of these two *n*-alkyl nitriles is similar to that observed for EtCN. For example, one series of reactions comprises over 75% of the final product ion intensity in the reaction of **1** with *n*BuCN. However, a new reaction pathway is available to *n*-alkyl nitriles with carbon chains longer than that of EtCN (Scheme II, path B).

The addition reaction sequence is observed for all nitriles investigated and leads to the products $Cp_2ZrC_{n+2}H_{2n+4}N^+$ (m/z 304, 318) and $Cp_2ZrC_{2n+3}H_{4n+5}N_2^+$ (m/z 373, 401) in the reaction of **1** with *n*PrCN and *n*BuCN (n = 3, 4), respectively (Scheme II, path A). The final ratios of m/z 304:m/z 373 and m/z 318:m/z 401 are 1.4 ± 0.3 and 2.4 ± 0.2, respectively.

CID of $Cp_2ZrC_{2n+2}H_{4n+3}N_2^+$ (m/z 359, 387) produces fragments $Cp_2ZrC_{n+1}H_{2n+2}N^+$ (m/z 290, 304) (eq 21), $Cp_2ZrC_nH_{2n-1}^+$

(20) Thorne, L. R.; Beauchamp, J. L. In *Gas Phase Ion Chemistry*; Bowers, M. T.; Ed.; Academic Press: New York, 1984; Vol. 3, p 41.
(21) Baykut, G.; Watson, C. H.; Weller, R. R.; Eyler, J. R. *J. Am. Chem. Soc.* **1985**, *107*, 8036.

(m/z 261, 275) (eq 22), and Cp_2ZrH^+ (m/z 221) (eq 23).

$$Cp_2ZrC_{2n+2}H_{4n+3}N_2^+ \xrightarrow{CID} \begin{cases} Cp_2ZrC_{n+1}H_{2n+2}N^+ + C_nH_{2n+1}CN & (21) \\ (m/z\ 290, 304) \\ C_nH_{2n+1}CN + H_3CN + Cp_2ZrC_nH_{2n-1}^+ & (22) \\ (m/z\ 359, 387) \qquad (m/z\ 261, 275) \\ Cp_2ZrH^+ + 2C_nH_{2n+1}CN & (23) \\ (m/z\ 221) \end{cases}$$

CID of $Cp_2ZrC_2H_4N^+$ (m/z 262) yields Cp_2ZrH^+ (m/z 221) as the only fragment ion other than Cp_2Zr^+. CID of $Cp_2ZrC_{n+1}H_{2n+2}N^+$ (m/z 290, 304) is consistent with spectra for high-energy CID of $Cp_2ZrC_{2n+2}H_{4n+3}N_2^+$ (m/z 359, 387).

The low yield of product ions $Cp_2ZrC_{n+2}H_{2n+4}N^+$ m/z 304, 318) complicates CID experiments, nevertheless it is clear both ions fragment to give $Cp_2ZrCH_3^+$ (m/z 235). In addition, $Cp_2ZrC_{n+1}H_{2n+2}N^+$ (m/z 304) also fragments to produce $Cp_2ZrC_2H_4N^+$ (m/z 262). CID experiments on m/z 330, 358 were unsuccessful due to the low abundance of these ions.

Increasing the internal energy of **1** affects the products formed in reactions with *n*PrCN and *n*BuCN. As the ionization energy is increased, the abundance of $Cp_2ZrC_nH_{2n+1}^+$ (m/z 263, 277) increases from 0 abundance to an amount approximately equal to the abundance of (m/z 261, 275) (eqs 24 and 25, Figure 4).

$$Cp_2ZrCH_3^+ + n\text{PrCN} \rightarrow Cp_2ZrC_3H_7^+ + CH_3CN \quad (24)$$

$$Cp_2ZrCH_3^+ + n\text{BuCN} \rightarrow Cp_2ZrC_4H_9^+ + CH_3CN \quad (25)$$

Discussion

Formation of $Cp_2ZrCD_3^+$. The reactivity of $Cp_2ZrCH_3^+$ toward nitriles in the gas phase is directly comparable to its solution reactivity. The main differences arise from the nature of ion/molecule interactions in the gas phase. The low frequency of third body collisions during the collision event allows the chemically activated collision complex[22,23] to sample a number of isomeric configurations before a collision, radiative decay, or decomposition removes excess internal energy. Precautions have been taken to insure observed reactions (other than CID) are exothermic or thermoneutral by addition of cyclohexane buffer gas (1×10^{-6}–5×10^{-6} Torr) and by using an appropriate thermalization time before reaction data are acquired, thus allowing some thermodynamic conclusions to be made.

With these conditions in mind, the reaction of $Cp_2ZrCH_3^+$ with CD_3CN to produce $Cp_2ZrCD_3^+$ may be understood (eq 8). A possible mechanism for the insertion/elimination reaction is given in Scheme III and is reminiscent of the mechanism proposed for insertion of alkenes and nitriles in solution.[1a,9,10,24,25] Precedence for the kinetic equivalency of the methyl groups is found in the NMR spectra of the isoelectronic $Cp^*_2ScN{=}C(CH_3)_2$, which shows identical methyl resonances.[10] The insertion of CD_3CN and elimination of CH_3CN yields products with no H/D scrambling indicating transfer of an intact CD_3 group. Thermalization of **1** occurs through collisions with buffer gas or substrate neutrals. When **1** is "hot" (nonthermal), it more efficiently undergoes the near thermoneutral process of CD_3CN insertion and CH_3CN elimination. This conclusion is supported by the reduced efficiency of $Cp_2ZrCD_3^+$ formation in the presence of a high pressure of buffer gas in conjunction with a low pressure of CD_3CN.

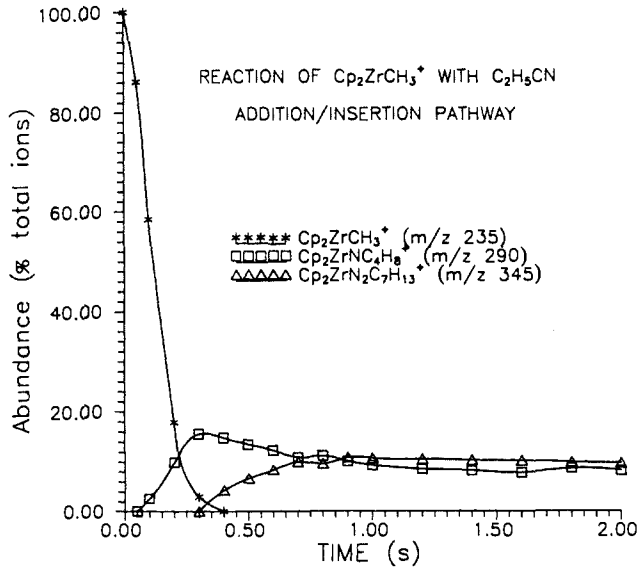

Figure 3. Ion abundance vs time for the addition pathway in the reaction of **1** with EtCN. Data are normalized to total ion abundance and fit with a cubic spline.

Scheme II

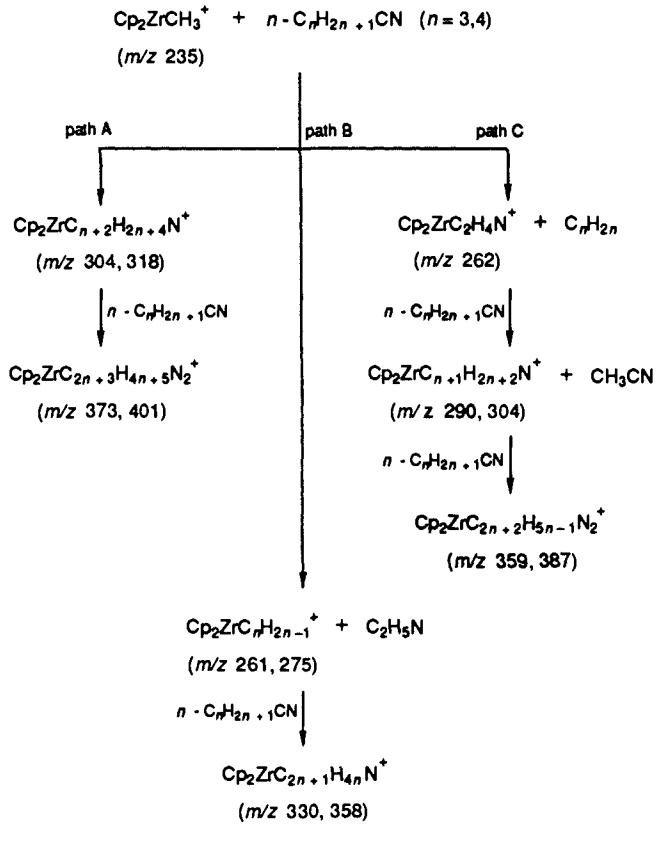

Reactions of $Cp_2ZrCH_3^+$ with CH_3CN. One interpretation of the results for this reaction (eqs 1 and 2) is that $Cp_2ZrCH_3^+$ adds one molecule of CH_3CN yielding two isomers with m/z 276 (eqs 26 and 27), $Cp_2ZrCH_3(N{\equiv}CCH_3)^+$ (**2**), and $Cp_2ZrN{=}C(CH_3)_2^+$ (**3**). To further explain the observations, only **3** is assumed to be reactive toward addition of a second acetonitrile molecule (eq 28).

Structures were assigned to the two isomers based on known solution structures and our gas-phase experimental results. Jordan et al. have reported similar product formation, i.e., the isolation of $Cp_2ZrCH_3(N{\equiv}CCH_3)^+$ as a BPh_4^- salt and the observation of $[Cp_2Zr(N{=}C(CH_3)_2)(N{\equiv}CCH_3)]^+$ detected by using NMR after irreversible acetonitrile insertion.[9] Recently, Bochmann et

(22) Robinson, P. J.; Holbrook, K. A. *Unimolecular Reactions*; Wiley-Interscience: New York, 1972.
(23) Forst, N. *Theory of Unimolecular Reactions*; Academic Press: New York, 1973.
(24) Jeske, G.; Lauke, H.; Mauermann, H.; Swepston, P. N.; Schumann, H.; Marks, T. J. *J. Am. Chem. Soc.* **1985**, *107*, 8091.
(25) Thompson, M. E.; Baxter, S.; Bulls, A. R.; Burger, B.; Nolan, N.; Santarsiero, B.; Schaefer, W.; Bercaw, J. *J. Am. Chem. Soc.* **1987**, *109*, 203.

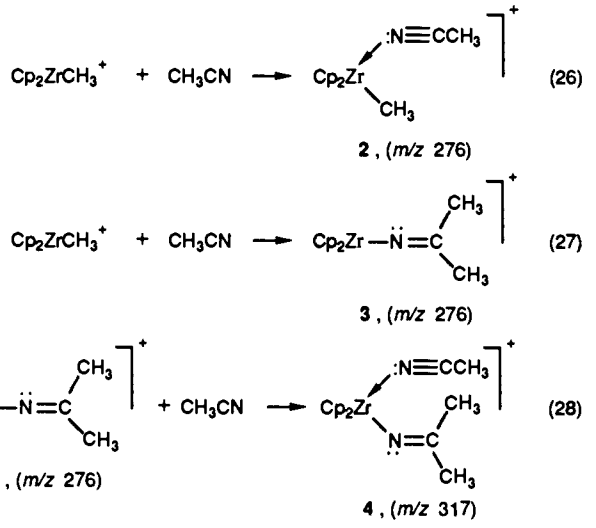

al. have investigated $Cp_2Ti(N{=}C(CH_3)_2)^+$ product formation by nitrile insertion for the cationic titanium analogue of **1**.[1b,c] Jordan and co-workers have also reported a bis-acetonitrile adduct $Cp_2ZrCH_3(N{\equiv}CCH_3)_2^+$; however, it is unlikely that this adduct is observed in the gas-phase due to its instability ($Cp_2ZrCH_3(N{\equiv}CCH_3)_2^+$ loses acetonitrile under mild conditions yielding $Cp_2ZrCH_3(N{\equiv}CCH_3)^+$).[9] Facile insertion of acetonitrile by $Cp^*_2ScCH_3$ leads to the formation of $Cp^*_2ScN{=}C(CH_3)_2$, and any further addition causes decomposition, presumably due to a reaction involving the Cp* rings.[10]

The structures proposed for the gas-phase products are analogous to structures reported for the nitrile adduct and insertion products of cationic Zr and Ti complexes.[1b,c,9] In addition, a number of experimental facts support the assignment of structurally isomeric products **2** and **3**. To aid in the discussion of the experimental observations, a qualitative potential energy surface for the proposed mechanism for the reaction of **1** with CH_3CN is given in Figure 5. Production of $[Cp_2Zr(N{=}C(CH_3)_2)(N{\equiv}CCH_3)]^+$ (m/z 317) from $Cp_2ZrN{=}C(CH_3)_2^+$ (m/z 276) does not proceed to completion (eq 2), and several different experiments show conclusively that these products are not in equilibrium. Isomeric products have been distinguished previously in ICR experiments by their reactivity differences.[26] In the present case the substrate CH_3CN is proposed to bind only to **3**. The observations may also be explained by addition of a second acetonitrile molecule to **2** with **3** inert to addition. However, steric considerations and results of other gas-phase reactions of **1**[27] support the addition occurring to the less hindered complex **3**.

The final ratio of m/z 276:m/z 317, 0.6, is then a measure of the ratio of nitrile adduct **2** and nitrile insertion product **3** in the total of m/z 276 ions produced (i.e., 37% of the total m/z 276 produced is stabilized as the adduct **2** and 63% as the insertion product). Product ions **2** and **3** would initially be formed as chemically activated species. Before a collision with a neutral or radiative cooling occurs **2** and **3** have internal energy in excess of the barrier for isomerization and therefore they interconvert rapidly. Rapid interconversion is substantiated by the observation of $Cp_2ZrCD_3^+$ (see above) and other deinsertion products discussed below. After thermalization at rates indicated by k_2 and k_3 in Figure 5, respectively, **2** and **3** are stabilized and no longer interconvert. Thus, m/z 276 intensity declines to a final value indicative of the amount of **2** present, and all of **3** is converted to $[Cp_2Zr(N{=}C(CH_3)_2)(N{\equiv}CCH_3)]^+$ (m/z 317), **4**, by addition of acetonitrile.

The low-energy CID-promoted conversion of m/z 276 to m/z 317 provides additional support for isomeric structures **2** and **3**. Low-energy translational excitation of **2** followed by collision converts some translational energy to internal energy sufficient to surmount the potential energy barrier for isomerization of **2**

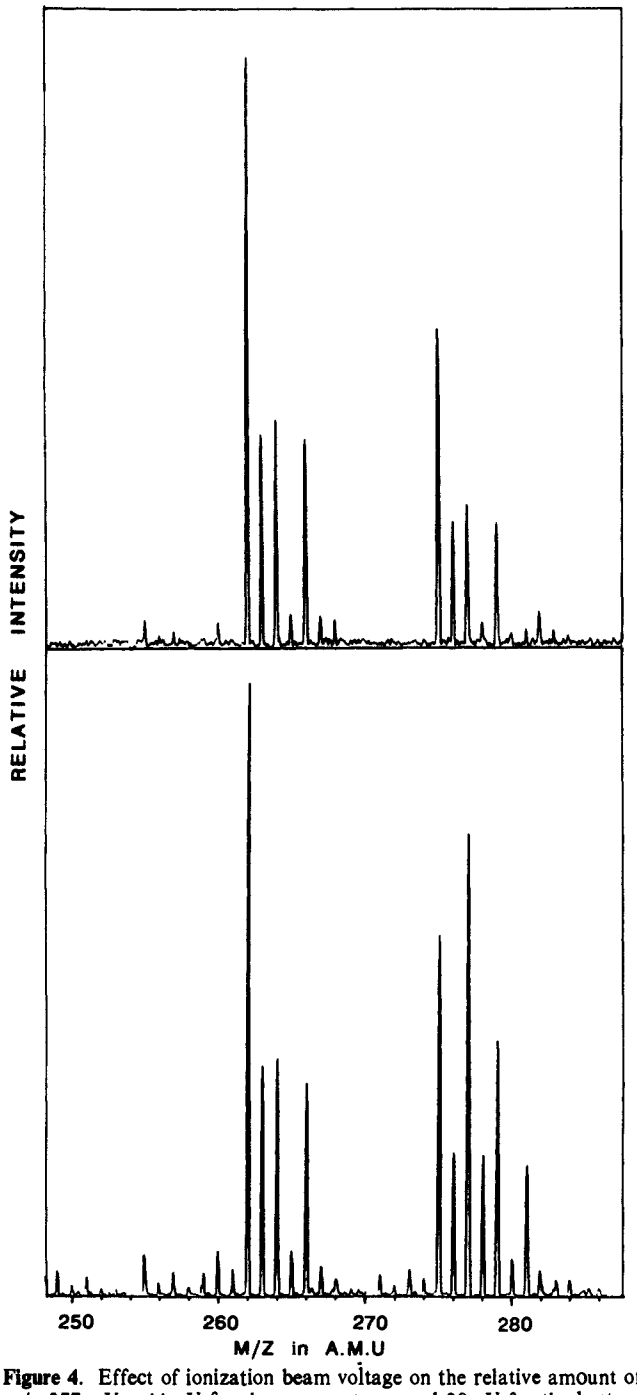

Figure 4. Effect of ionization beam voltage on the relative amount of m/z 277. V = 11 eV for the top spectrum and 30 eV for the bottom spectrum. Essentially no m/z 277 is formed in the 11-eV spectrum. Note the increase in the major ^{90}Zr peak at m/z 277 for the 30-eV spectrum.

to **3** *without fragmenting the* m/z 276 ion. The collision complex formed by collision with buffer gas or substrate directly after low-power irradiation of unreactive **2** apparently has internal energy above the isomerization barrier but *below* the Zr–N dissociative barrier, and a rearrangement may occur before a colliding neutral or radiative cooling removes energy following dissociation of the collision complex. The result is isomerization followed by addition of CH_3CN to **3**, which is observed as an increase in the intensity of $[Cp_2Zr(N{=}C(CH_3)_2)(N{\equiv}CCH_3)]^+$ **4** (eq 28).

It is apparent from CID experiments on m/z 276 (eqs 6 and 7) that the isomerization of **3** to **2** and loss of CH_3CN is more facile than cleavage of the $Zr{-}N{=}C(CH_3)_2$ bond. Rearrangements caused by CID are not uncommon.[16a,28] The CID

(26) Allison, J. *Prog. Inorg. Chem.* **1986**, *34*, 627.
(27) Armentrout, P.; Beauchamp, J. *Acc. Chem. Res.* **1989**, *22*, 315.
(28) Jacobson, D. B.; Freiser, B. S. *J. Am. Chem. Soc.* **1983**, *105*, 5197.

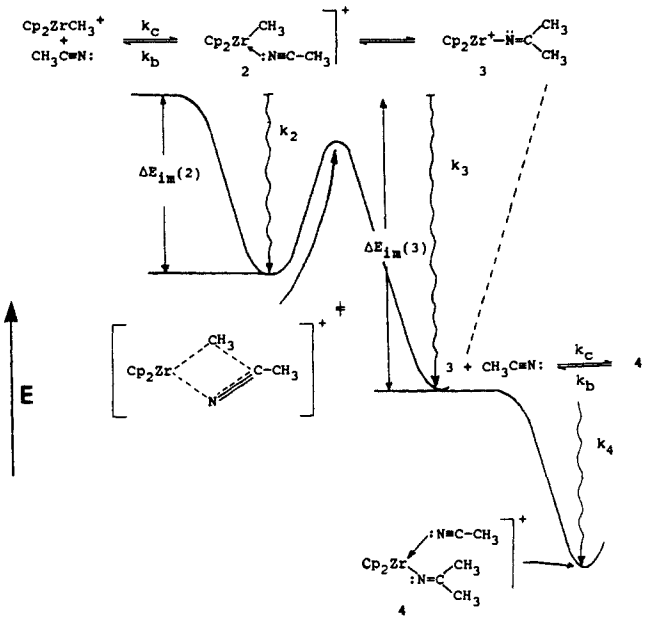

Figure 5. Qualitative gas-phase potential surface describing the reaction of **1** with CH_3CN. Symbols are defined in the text.

Scheme III

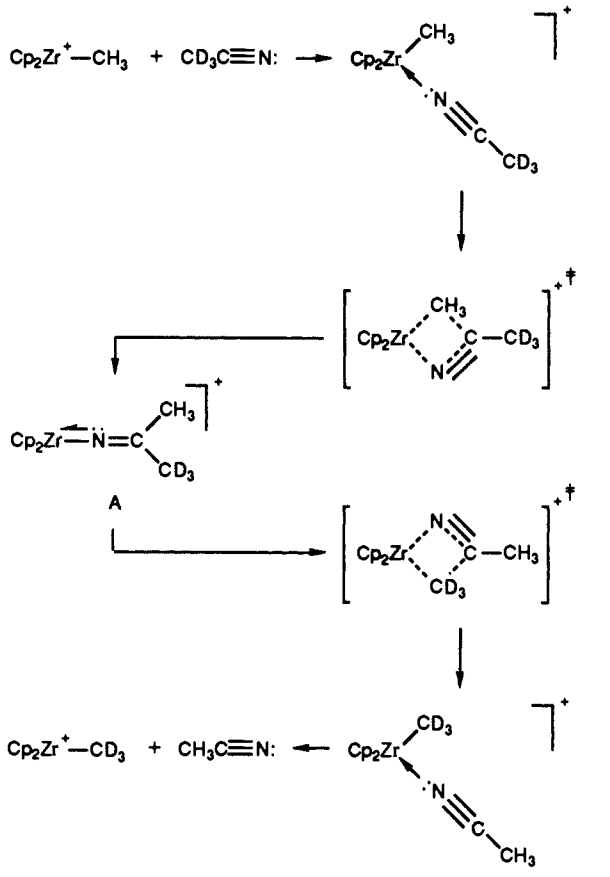

results are consistent with interconvertible isomeric structures **2** and **3** because the observed loss of stable neutral CH_3CN would be expected rather than loss of the neutral radical fragment $^{\bullet}N{=}C(CH_3)_2$.

CID of m/z 317 (eqs 3–5) indicates that loss of CH_3CN is the most facile fragmentation pathway at low CID energies. This result is consistent with the simple nitrile adduct structure $[Cp_2Zr(N{=}C(CH_3)_2)(N{\equiv}CCH_3)]^+$ but does not exclude the possibility of a metalloheterocycle structure similar to that reported by Bercaw and co-workers in the $Cp^*_2ScCH_3$ system.[10] However, $Cp_2ZrCH_3(N{\equiv}CCH_3)^+$ and $Cp_2TiCH_3(N{\equiv}CCH_3)^+$ both insert CH_3CN to produce $Cp_2ZrN{=}C(CH_3)_2(N{\equiv}CCH_3)^+$ and $Cp_2TiN{=}C(CH_3)_2(N{\equiv}CCH_3)^+$, respectively, in solution.[1,9] Therefore, the logical choice for the proposed structure of **4** is $[Cp_2Zr(N{=}C(CH_3)_2)(N{\equiv}CCH_3)]^+$.

Reaction of $Cp_2ZrCH_3^+$ with *t*BuCN. The reaction of **1** with *t*BuCN (eqs 10 and 11) resembles the reaction of **1** with CH_3CN, and eqs 29–31 account for the observations. Initial reaction of *t*BuCN with **1** gives two isomers with m/z 318, a simple adduct, $Cp_2ZrCH_3(N{\equiv}C(t\text{Bu}))^+$ (**5**), and the insertion product, $Cp_2ZrN{=}C(CH_3)(t\text{Bu})^+$ (**6**) (eqs 29 and 30). Additional coordination of *t*BuC≡N to **6** yields $[Cp_2Zr(N{=}C(CH_3)(t\text{Bu}))(N{\equiv}C(t\text{Bu}))]^+$, **7** (eq 31), and the ratio of **5** to **7** is 5.5 ± 0.1.

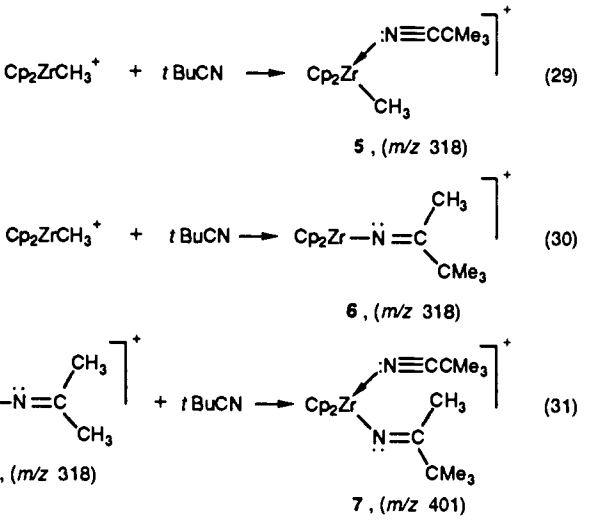

This ratio may be interpreted to indicate that the simple adduct, **5**, constitutes 85% of the total m/z 318 formed, and 15% is the insertion product, **6**. The relative amount of the simple adduct **5** formed for this substrate is larger than for CH_3CN, where **2** is approximately 40% of the total m/z 276. Depending on the mechanism of thermalization for adduct formation (see below), this increase may be explained by changes in the relative stabilities of the simple adduct vs the insertion product or changes in the thermalization rates or both.

$Cp_2ZrC(CH_3)_3^+$ was not observed under any circumstances, even as ionization energy for producing $Cp_2ZrCH_3^+$ was raised to 70 eV forming "hot" $Cp_2ZrCH_3^+$. This negative result may arise from a high barrier for migration of the $C(CH_3)_3$ group or because of a low $Zr{-}C(CH_3)_3$ bond disruption enthalpy relative to $Zr{-}CH_3$ (leading to a substantially endothermic reaction). Furthermore, $Cp_2ZrC(CH_3)_3^+$ was not formed in CID experiments (eqs 12 and 13). This strongly supports structure **5** as the adduct m/z 318, since no evidence for deinsertion or formation of the isomeric structure $[Cp_2ZrC(CH_3)_3(N{\equiv}CCH_3)]^+$ has been obtained.

Reactions of $Cp_2ZrCH_3^+$ with PhCN. Two reaction sequences are observed for reaction of **1** with PhCN. The major pathway is assumed to begin with insertion of PhCN and elimination of CH_3CN, resulting in the formation of Cp_2ZrPh^+ (m/z 297) (eq

$$\underset{(m/z\ 235)}{Cp_2ZrCH_3^+} + PhCN \rightarrow \underset{(m/z\ 297)}{Cp_2ZrPh^+} + CH_3CN \quad (32)$$

32). The formation of Cp_2ZrPh^+ must be exothermic or near thermoneutral since ion/molecule reactions endothermic by more than a few kcal/mol are not usually observed in the FTICR method when ions are thermalized. Furthermore, no reduction in its abundance is observed when high buffer gas pressure is present during the reaction, suggesting that nonthermal ions are not responsible for the reaction. The fundamental transformations in eqs 33a–c may be used to obtain a lower limit for the Zr–Ph bond disruption enthalpy relative to the $Zr{-}CH_3$ bond disruption enthalpy (assuming negligible entropy changes). Since the reaction represented in eq 32 is observed, the Cp_2Zr^+–Ph bond disruption

Scheme IV

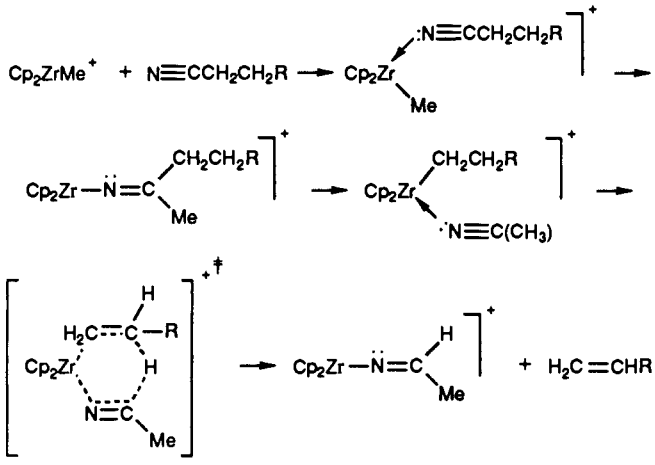

Scheme V

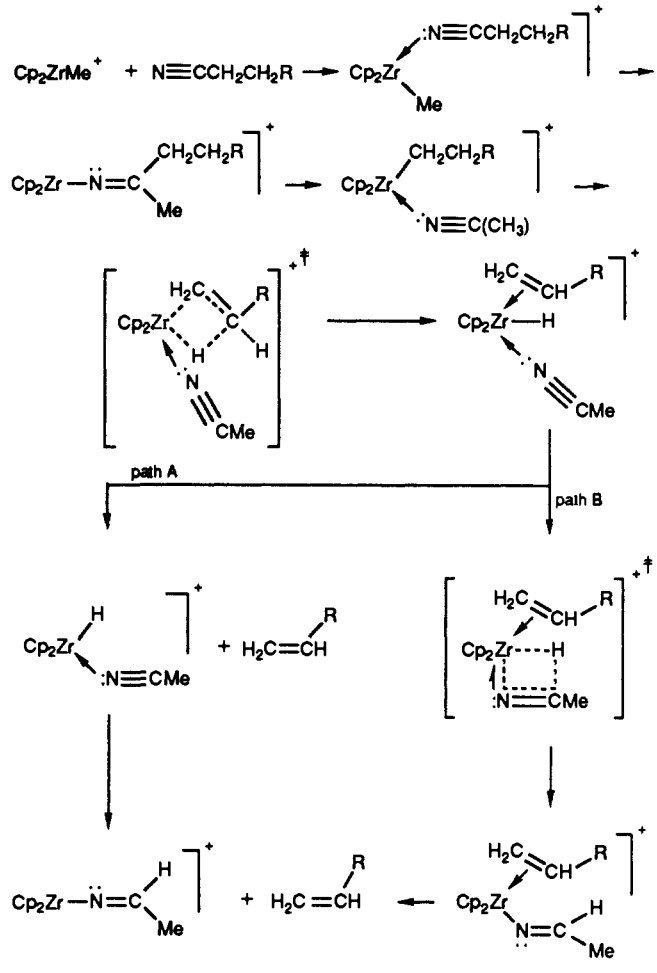

enthalpy must be greater than the Cp_2Zr^+–CH_3 bond disruption enthalpy by > ca. 8 kcal/mol.[29]

$$Cp_2ZrCH_3^+ \rightarrow Cp_2Zr^+ + {}^\bullet CH_3 \quad BDE_1 \quad (33a)$$

$${}^\bullet CH_3 + PhCN \rightarrow {}^\bullet Ph + CH_3CN \quad \Delta H' = 8 \pm 2 \text{ kcal mol}^{-1} \quad (33b)$$

$$Cp_2Zr^+ + {}^\bullet Ph \rightarrow Cp_2ZrPh^+ \quad -BDE_2 \quad (33c)$$

$$Cp_2ZrCH_3^+ + PhCN \rightarrow Cp_2ZrPh^+ + CH_3CN \quad BDE_1 + \Delta H' - BDE_2 < 0 \quad (34)$$

The reaction of Cp_2ZrPh^+ with PhCN (eqs 15 and 16) indicates that the adduct $Cp_2ZrPh(N{\equiv}CPh)^+$ (m/z 400), **8**, and the insertion product $Cp_2ZrN{=}CPh_2^+$ (m/z 400), **9**, are both produced (eqs 35 and 36). Addition of PhCN to **9** occurs giving $[Cp_2Zr(N{=}CPh_2)(N{\equiv}CPh)]^+$, **10** (eq 37), and the ratio of the abundance of **8** to **9** is reflected in the final ratio of **8** to **10**, 0.3 ± 0.1. Therefore, **8** represents approximately 25% of the total m/z 400 ion population.

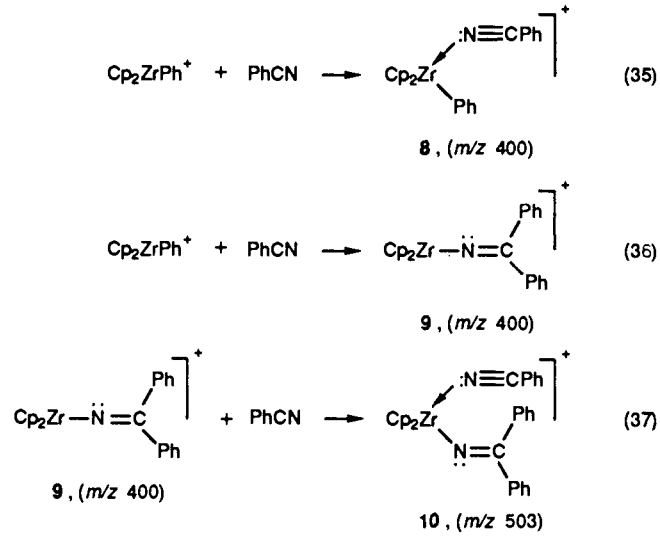

The minor pathway in the reaction of **1** with PhCN is similar to reaction sequences observed for CH_3CN and *t*BuCN. Addition of PhCN to **1** produces both the adduct $Cp_2ZrCH_3(N{\equiv}CPh)^+$, ($m/z$ 338) **11**, and the insertion product $Cp_2ZrN{=}C(CH_3)(Ph)^+$ (m/z 338), **12**, and only **12** reacts further to form $Cp_2ZrN{=}C(Ph)(CH_3)(N{\equiv}CPh)^+$, **13** ($m/z$ 441) (eqs 38, 39, and 40).

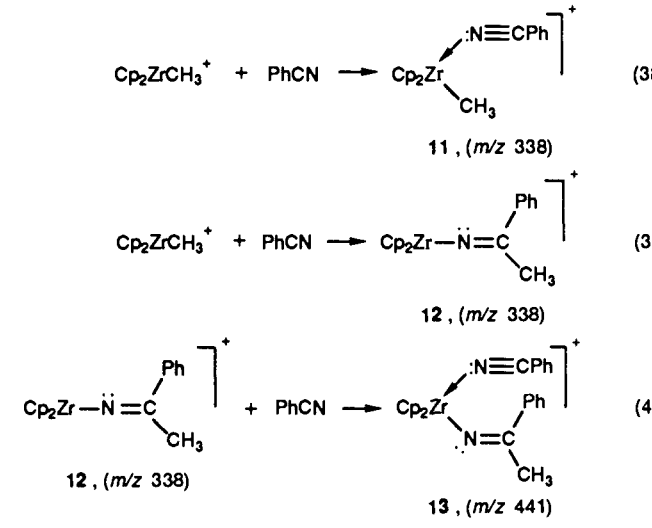

The assignment of structures **11** and **13** is complicated by their low abundance, which precludes obtaining reliable CID spectra. Therefore, isomeric structures **14** and **15** are also possible products. The relative ease of Ph migration evidenced by the abundance of Cp_2ZrPh^+ formed indicates that m/z 338 is probably a mixture of isomers **11** and **14**. Formation of isomer **15** is less likely than

(29) All thermodynamic values were derived from enthalpies of formation obtained from the following sources: (a) Cox, J. D.; Pilcher, G. *Thermochemistry of Organic and Organometallic Compounds*; Academic Press: London, 1970. (b) Lias, S. G.; Bartmess, J. E.; Liebman, J. F.; Holmes, J. L.; Levin, R. D.; Mallard, G. W. *Gas-Phase Ion and Neutral Thermochemistry*; American Chemical Society and The American Institute of Physics for The National Bureau of Standards: New York, 1988. (c) Lowry, T. H.; Richardson, K. S. *Mechanisms and Theory in Organic Chemistry*; Harper and Row, Publishers: New York, 1987; p 483. (d) Pedley, J. B.; Naylor, R. D.; Kirby, S. P. *Thermochemical Data of Organic Compounds*; Chapman and Hall: New York, 1986.

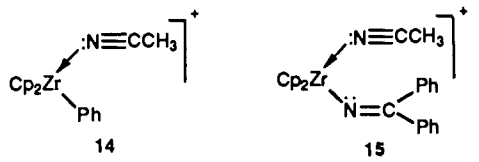

14 15

formation of **13** since significant rearrangement is required after coordination of PhCN to **12**.

Reaction of $Cp_2ZrCH_3^+$ with *n*-Alkyl Nitriles. *The alkene elimination pathway.* The reactions of **1** with *n*-alkyl nitriles exhibit some reaction sequences not observed for CH_3CN, Me_3CCN, and PhCN. A common feature in the reactions of the three *n*-alkyl nitriles investigated is the production of $Cp_2ZrC_2H_4N^+$ (m/z 262) accompanied by the loss of an alkene (eq 41). The azomethine structure $Cp_2ZrN{=}C(H)(CH_3)$, **16**,

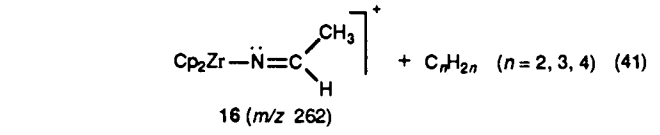

16 (m/z 262)

is most likely for m/z 262. Similar insertion products generated from organometallic hydrides have been synthesized, and, in contrast to organometallic alkyls, no observation of a stable intermediate adduct was reported, suggesting a facile insertion.[8,10]

The mechanisms in Schemes IV and V are both consistent with experimental observations. Scheme IV is similar to the mechanism proposed for the loss of alkenes from higher alkyl aluminum nitrile adducts upon heating.[30] The first step in Scheme IV involes nitrile coordination followed by insertion. Subsequent deinsertion produces an acetonitrile adduct that undergoes transfer of a β-hydrogen to the azomethine carbon. The final product results from elimination of the corresponding alkene through a six-membered transition state.

Scheme V is an alternative mechanism that does not directly involve coordinated acetonitrile in the loss of alkene. This mechanism is similar to β-hydride shift/alkene elimination, which is used to describe elimination of alkene in the polymerization of unsaturated hydrocarbons by electron-deficient metal complexes in solution.[31] In this case, after insertion/deinsertion, transfer of a β-hydrogen to the metal center is followed by insertion of CH_3CN and elimination of alkene (path A or B). If path A in Scheme V is indeed operative, it is noteworthy that β-hydride shift/alkene elimination occurs for the Zr-alkyl intermediate when the nitrile is bound, as occurs in the solution chemistry of the cation. In contrast, "unsolvated" $Cp_2Zr(alkyl)^+$ complexes decompose by β-hydride shift/dehydrogenation in the gas phase.[14a,b] Thus, the presence of the inner-sphere nitrile may simulate the role of solvent in directing the chemistry of these electrophilic complexes.

According to the proposed mechanisms, Schemes IV and V, insertion/deinsertion and β-hydride shift are required for alkene elimination in the reactions of **1** with nitriles. The insertion/deinsertion step is supported by a number of observations. The formation of $Cp_2ZrCD_3^+$ and Cp_2ZrEt^+ are observed in the reactions of $Cp_2ZrCH_3^+$ with CD_3CN, eq 8, and EtCN, Scheme I, respectively. In addition, both $Cp_2ZrC_3H_7^+$ and $Cp_2ZrC_4H_9^+$ are produced from the reactions of "hot" $Cp_2ZrCH_3^+$ with C_3H_7CN and C_4H_9CN, respectively (eqs 24 and 25). Furthermore, trimethylacetonitrile is the only alkyl nitrile that shows no aptitude for deinsertion (i.e., formation of $Cp_2Zr{-}C(CH_3)_3^+$ is not observed even in the reaction of "hot" **1** with *t*BuCN). Elimination of alkene is observed in the reactions of **1** with *n*-$C_nH_{2n+1}CN$ (n = 2, 3, 4) where insertion/deinsertion is known to occur, and elimination of isobutene is known for the reaction of $Al(C(CH_3)_3)_3$ with nitriles in solution and is expected in the reaction of **1** with *t*BuCN. However, since deinsertion is not observed in the reaction of **1** with *t*BuCN (vide infra), isobutene elimination does not occur. These results also strongly suggest that elimination of alkenes will not occur in reactions of electrophilic d^0f^n metal-methyl and hydride complexes with nitriles in solution, since reported nitrile insertion is irreversible in the condensed phase.

The next step in the alkene elimination sequence is the conversion of **16** to $Cp_2ZrN{=}C(H)(C_nH_{2n+1})^+$ (n = 2, 3, 4), **17**.

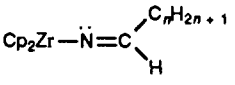

17

Bercaw and co-workers have reported a similar exchange in which *p*-anisonitrile displaces *t*BuCN from $Cp^*_2ScN{=}C(H)C(CH_3)_3$.[10] Attempts to displace *t*BuCN from $Cp^*_2ScN{=}C(H)C(CH_3)_3$ with CH_3CN lead to decomposition; therefore, the relative magnitude of steric and electronic effects could not be determined. The displacement of CH_3CN by $C_nH_{2n+1}CN$ (n = 2, 3, 4) in the gas phase indicates that electronic effects are evidently more important than steric effects for the *n*-alkyl nitriles studied here.

The structure of **17** is corroborated by the final step in the alkene elimination pathway. Complete conversion of **17** to $[Cp_2Zr(N{=}C(H)(C_nH_{2n+1}))(N{\equiv}CC_nH_{2n+1})]^+$ (n = 2, 3, 4), **18**, supports the assignment of an azomethine insertion isomer. However, the steric requirements for hydrogen are small, so the possibility of a bis-nitrile adduct cannot be completely dismissed.

The formation of Cp_2ZrEt^+ in the reaction of **1** with EtCN leads to the calculation of a lower limit for the relative Zr^+–Et bond disruption enthalpy (eq 42).[29] The small enthalpy change calculated for eq 42 indicates that the Zr^+–Et bond disruption enthalpy is comparable to or greater than the Zr^+–CH_3 bond disruption enthalpy. By analogy to related complexes,[25,37] an agostic interaction may be present in the ethyl complex and could account for the surprisingly high Zr–Et bond energy relative to Zr–Me.

$$^{\bullet}CH_3 + :N{\equiv}C\text{-}Et \rightarrow {}^{\bullet}Et + :N{\equiv}CCH_3 \qquad (42)$$

$$\Delta H_{42} = -1 \text{ kcal mol}^{-1}$$

Formation of Allyl Cations. The structures of m/z 261 and m/z 275 in Scheme II (path B) are assigned as allyls. The observation of allyl species in reactions of **1** with *n*PrCN and *n*BuCN is not unexpected. Allyl cations are generated readily in the reactions of **1** with a variety of alkenes.[14a,b] The mechanism for this transformation is probably similar to that proposed for the alkene reactions.[14a,b] However, the neutral molecules eliminated upon Zr–allyl formation have not been identified. Two obvious possibilities are H_2 and CH_3CN or the imine $CH_3CH{=}NH$ (both possibilities are covered by the "C_2H_5N" eliminated in Scheme II, path B). An estimate for the enthalpy of the reaction eliminating H_2 and CH_3CN can be obtained by neglecting the zirconium–carbon bond disruption enthalpies (eq 43). If H_2 and CH_3CN are produced, the Zr^+–allyl bond disruption enthalpy must be at least ~15 kcal mol^{-1} stronger than the Zr^+–CH_3 bond disruption enthalpy.[29] One possible mechanism for generating the allyl complex by elimination of CH_3CN and H_2 is directly analogous to that proposed for elimination of H_2 in the reaction of **1** with ethylene.[14a,b] Insertion/deinsertion yields $Cp_2ZrC_3H_7(N{\equiv}CCH_3)^+$, and acetonitrile must remain coordinated to the metal center during the dehydrogenation and eliminated subsequent to allyl formation. Without acetonitrile coordination, the β-hydride shift required for allyl formation is endothermic and will not occur.

$$^{\bullet}CH_3 + C_3H_7CN \rightarrow {}^{\bullet}C_3H_5 + H_2 + CH_3CN \qquad (43)$$

$$\Delta H_{43} = 15.2 \text{ kcal mol}^{-1}$$

Calculation of the enthalpy for the reaction eliminating $CH_3CH{=}NH$ yields a value of approximately 2 kcal mol^{-1} (eq 44)[29] and provides little information concerning the Zr^+–allyl bond

$$^{\bullet}CH_3 + C_3H_7CN \rightarrow {}^{\bullet}C_3H_5 + CH_3{-}CH{=}NH \qquad (44)$$

$$\Delta H_{44} \cong 2 \text{ kcal mol}^{-1}$$

(30) Sonnek, G.; Baumgarten, K. G.; Reinheckel, H.; Pasynkiewicz, S.; Starowieyski, K. B. *J. Organomet. Chem.* **1978**, *150*, 21.
(31) Jordan, R. F. *J. Chem. Ed.* **1988**, *65*, 285.

Scheme VI

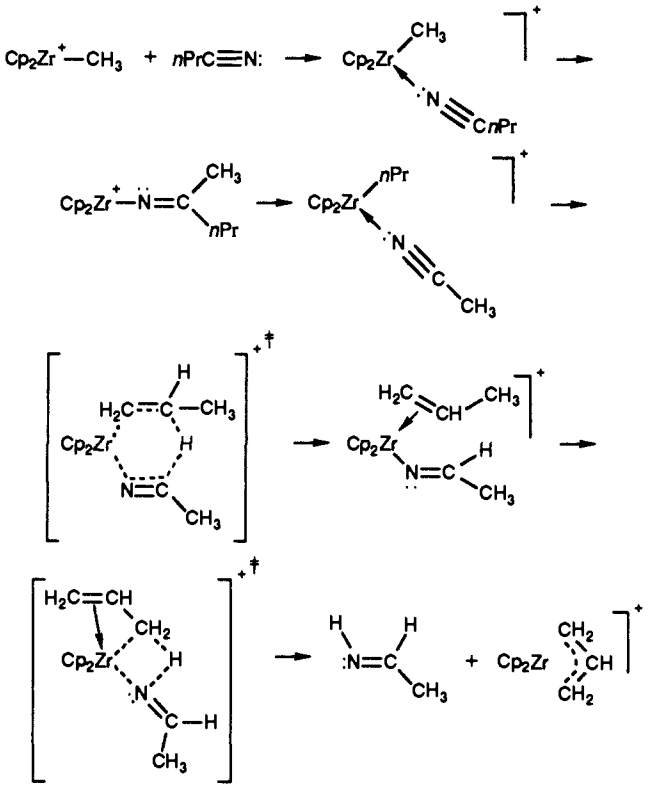

strength. Elimination of the imine is thermodynamically more favorable than elimination of acetonitrile and H_2. A mechanism for formation of the Zr^+–allyl complex by elimination of imine in the reaction of **1** with C_3H_7CN is shown in Scheme VI. Insertion/deinsertion precedes formation of a zirconium azomethine propene complex. Allylic C–H activation yields the allyl complex, $Cp_2ZrC_3H_5^+$, with elimination of $HN{=}CHCH_3$. Catalytic hydrogenation of nitriles to amines has been demonstrated but is proposed to involve H–H rather than C–H activation.[10] The C–H activation process is similar to the final step proposed for elimination of H_2 in the reaction of **1** with ethylene.[14a]

The Addition/Elimination Pathway. The addition of *n*-$C_nH_{2n+1}CN$ (n = 2, 3, 4) to **1** can occur producing both the adduct isomer $Cp_2ZrCH_3(N{\equiv}CC_nH_{2n+1})^+$, **19**, and the insertion isomer

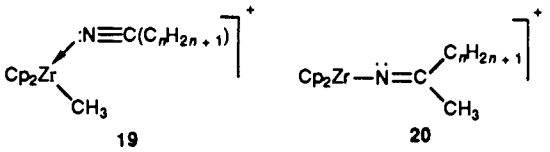

19 **20**

$Cp_2ZrN{=}C(CH_3)(C_nH_{2n+1})^+$, **20**. However, another structural isomer is possible, $Cp_2ZrC_nH_{2n+1}(N{\equiv}CCH_3)^+$, **21**. Since Cp_2ZrEt^+ reacts with EtCN to produce $Cp_2ZrN{=}C(H)(Et)^+$ and eliminate ethylene, it is unlikely that isomer **21** is produced in significant yield.

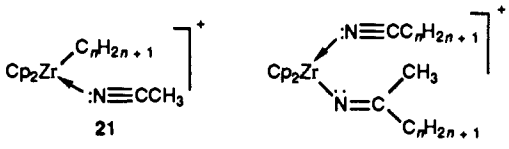

21 **22**

Cation **20** reacts further to produce $[Cp_2Zr(N{=}C(CH_3)(C_nH_{2n+1}))(N{\equiv}CC_nH_{2n+1})]^+$, **22** ($n$ = 2, 3, 4), and the final ratio of **19**:**22** may be compared to analogous final ratios for the *t*BuCN and CH_3CN systems giving the following order: CH_3CN (0.6 ± 0.1), EtCN (0.8 ± 0.1), *n*PrCN (1.4 ± 0.3), *n*BuCN (2.4 ± 0.2), *t*BuCN (5.5 ± 0.1). Thermodynamic parameters for the addition/insertion pathway are not known, but the more basic nitriles appear less likely to insert in this chemistry. The relative order is also consistent with steric factors determining the relative stability of simple adducts vs insertion products. Beyond these observations, insufficient evidence is available to define the reasons for the trend.

Kinetics of Formation of Nitrile Adducts. The efficient formation of adducts where one or two nitrile molecules are coordinated without subsequent elimination of a neutral molecule was somewhat surprising (eqs 26–28, 29–31, 35–37, 38–40). For eq 26/27 the efficiency of formation of m/z 276 is $k_f/k_{ADO} \approx$ 0.05–0.15. The observation of ions at m/z 276 occurs only as a consequence of removal of the internal energy of the chemically activated collision complexes.[21,22] These complexes have minimum internal energies before cooling equal to the reduction in potential energy upon their formation (ΔE_{im} in Figure 5). If the cooling occurs via third-body collisions, the kinetic scheme in eq 45 applies (for eq 26)

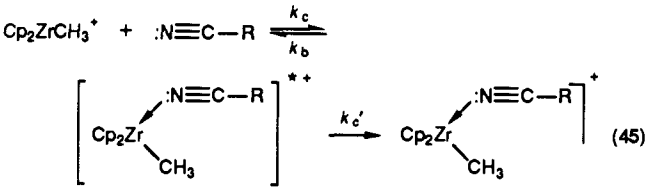

(45)

where k_c and k_c' are second-order collision rate constants, and k_b is the unimolecular decomposition rate constant for the chemically activated complex. For eq 45, the overall efficiency, k_f/k_c, equals $k_c'[B]/(k_c'[B] + k_b)$, which is the branching ratio for the chemically activated complex. If the efficiency is ≈0.05, k_c and $k_c' = 10^{-9}$ cm^3 s^{-1} (strong collision limit[33a]), and [B] = 2 × 10^{-6} Torr, then $k_b \approx 1 \times 10^3$ s^{-1}.[34] This k_b value represents a lifetime for the chemically activated complex of ≈1 ms. The large value for the lifetime of the collision complex implies a large value for ΔE_{im} in conjunction with the large number of degrees of freedom in the cyclopentadienyl complex.[22]

Alternatively, highly efficient radiative cooling may be occurring to stabilize the collision complex. Studies relevant to the present system have been summarized by Caldwell and Bartmess.[35] They investigated adduct formation in the reactions of alcohols with alkoxide anions in an ICR spectrometer. Radiative emission is indicated by a pressure independent rate coefficient for adduct formation (i.e., altering the value of $k_c'[B]$ in eq 45 has no effect). The second-order rate constant for formation of $Cp_2ZrC_3H_6N^+$, m/z 276 (eq 1), is estimated to be one order of magnitude less than the ADO collisional rate constant. Only a small increase in the rate constant is observed upon addition of inert buffer gas (P_{buffer} = 0–1.5 × 10^{-5} Torr). The relative absence of pressure dependence observed in this work is consistent with substantial radiative cooling as a mechanism for adduct formation.

Conclusions

The reactions of $Cp_2ZrCH_3^+$ with nitriles in the gas phase show features of the reactions of similar cationic and neutral transition-metal alkyl and hydride complexes as well as aluminum alkyls with nitriles in solution.

A summary of the reactivity of **1** and various nitriles is given in Figure 6. Essentially four major reaction pathways are observed. One reaction sequence is common to all nitriles investigated and involves the formation of two isomers (path A in Figure 6). The addition of nitrile to **1** generates a nitrile adduct isomer, and subsequent insertion forms the azomethine insertion product. Both isomers are produced in all cases and are distinguished by their further facile reactions with nitrile substrate. Simple nitrile adducts of **1** are inert to detectable reaction with substrate, and the insertion products react by addition of a second equivalent of nitrile. This constitutes the only reaction pathway observed for

(32) (a) Schock, L. E.; Marks, T. J. *J. Am. Chem. Soc.* **1988**, *110*, 7701. (b) Bruno, J. W.; Marks, T. J.; Morss, L. R. *J. Am. Chem. Soc.* **1983**, *105*, 6824.

(33) (a) Olmstead, W. N.; Lev-On, M.; Golden, D. M.; Brauman, J. I. *J. Am. Chem. Soc.* **1977**, *99*, 992. (b) Jasinski, J. M.; Rosenfeld, R. N.; Golden, D. M.; Brauman, J. I. *J. Am. Chem. Soc.* **1979**, *101*, 2259.

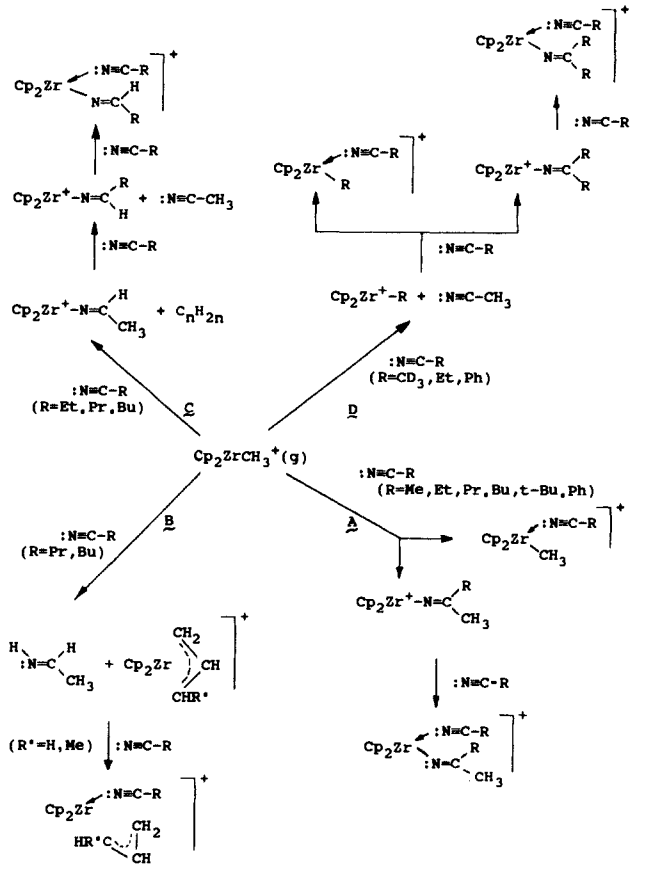

Figure 6. Reactivity summary for reactions of **1** with the nitriles investigated here.

CH_3CN and *t*BuCN. For labeled acetonitrile, cyanobenzene, and EtCN, insertion/deinsertion exchanges the R group on the metal, and the resulting complex reacts further to add 1 and 2 equiv of nitrile (path D in Figure 6). Lower limits on the Zr^+–Ph and Zr^+–Et bond disruption enthalpies relative to Zr^+–CH_3 have been calculated assuming the formation of Cp_2ZrPh^+ and Cp_2ZrEt^+ is exothermic or thermoneutral (path D in Figure 6). CID experiments present no evidence for the formation of metalloheterocycles in any of the nitriles studies. However, a metalloheterocyclic structure cannot be ruled out.

The third reaction pathway begins with insertion of *n*-alkyl nitrile followed by loss of the olefin C_nH_{2n} and formation of $Cp_2ZrN{=}C(H)(CH_3)^+$ (path C in Figure 6). A six-membered transition state, similar to that proposed for elimination of alkenes in the reactions of nitriles with higher aluminum alkyls, may be used to describe this transformation. However, it may also be viewed as a β-hydride shift/alkene elimination, which in this case is related to the presence of the inner-sphere nitrile, which may sterically inhibit the dehydrogenation pathway observed exclusively in the gas-phase chemistry of $Cp_2Zr(alkyl)^+$ cations.[14a,b] Displacement of CH_3CN from $Cp_2ZrN{=}C(H)(CH_3)^+$ by *n*-$C_nH_{2n+1}CN$ (n = 2, 3, 4) occurs for all three nitriles. Finally, addition of *n*-$C_nH_{2n+1}CN$ to $Cp_2ZrN{=}C(H)(C_nH_{2n+1})^+$ proceeds to completion, thus the formation of a hydride–nitrile adduct is not necessary to accurately describe this reaction sequence.

Finally, path B in Figure 6 shows the production of Zr–allyl complexes in the reaction of **1** with higher alkyl nitriles. The CID behavior of these product ions suggests that they are equivalent to the allyl complexes produced in the reactions of **1** with alkenes.[14a,b] A single nitrile can add to these allyl products.

Significantly, the reactivity of **1** toward nitriles in the gas phase indicates that many of the processes observed in solution for **1** and similar complexes can be studied in detail in the absence of solvent, providing a different but comparable perspective on the reactivity of d^0 cationic complexes. Few comparative studies of this kind have been reported. The results herein are indicative of the possibilities for investigating other organometallic systems in the gas phase and suggest that insights into the synthesis of organometallic species and their reactivities with a variety of substrates may be probed without interference from solvent. The results from gas-phase studies may then be successfully applied to solution chemistry as long as the inherent differences in the two phases are understood.

Experimental Section

Results for ion/molecule reactions of **1** with nitriles were obtained by using a Nicolet FTMS 1000 ion cyclotron resonance mass spectrometer. Electron impact (EI) (11–12 eV) on $Cp_2Zr(CH_3)_2$ ($p \approx 10^{-8}$–10^{-7} Torr) yields predominantly $Cp_2ZrCH_3^+$ and $Cp_2Zr^{\bullet+}$. $Cp_2Zr^{\bullet+}$ and any substrate ions formed during EI are ejected from the ICR cell by using a RF pulse, thereby isolating **1** for ion/molecule reaction studies with nitriles ($p = 5 \times 10^{-7}$–1×10^{-5} Torr). Ejection of all ions other than **1** prevents charge-transfer reactions from reforming $Cp_2Zr^{\bullet+}$, which forms adducts with nitriles and can confuse the interpretation of mass spectra. Binuclear zirconium ion formation limits the study of ion/molecule reactions to those with rate constants greater than 1×10^9 M^{-1} s^{-1} (1×10^{-12} cm^3 s^{-1}); therefore, it is advantageous to keep $Cp_2Zr(CH_3)_2$ pressure below 5×10^{-8} Torr to minimize the loss of $Cp_2ZrCH_3^+$ from this side reaction. The abundance of **1** is also depleted by its reaction with even trace amounts of water (eq 46), therefore drying of all substrates is imperative.

$$Cp_2ZrCH_3^+ + H_2O \rightarrow Cp_2ZrOH^+ + CH_4 \qquad (46)$$

The final ratios for the reaction of **1** with nitriles were determined from at least seven measurements, and 95% confidence limits are included.

All nitriles studied were purchased from commercial sources in high purity and dried over CaH_2. Distillation of benzonitrile from CaH_2 was necessary to remove water. $Cp_2Zr(CH_3)_2$ and $Cp_2Zr(CD_3)_2$ were synthesized from a literature preparation, and satisfactory analysis was obtained by NMR and mass spectrometry.[36] Deuteromethyllithium was synthesized in dry diethyl ether from CD_3I, which was purchased from Aldrich. $Cp_2Zr(CD_3)_2$ was found to be at least 99% deuterated by mass spectrometric analysis.

Pressures reported in the text are read directly from an ionization gauge and are approximate except for those reported for kinetic experiments, which are derived from calibration experiments employing a baratron capacitance manometer.[14b] In other experiments the pumping speed was limited so that the pressure read from the ionization gauge was as close as possible to the actual pressure in the ICR cell.[14b] Rate coefficients reported in the text include 95% confidence limits and are determined from at least three measurements.

Acknowledgment. Support for this work was provided by grants from the National Science Foundation (CHE-8700765), which is gratefully acknowledged. We also thank R. F. Jordan and J. I. Brauman for helpful discussions.

Registry No. $Cp_2ZrCH_3^+$, 94370-49-7; CH_3CN, 75-05-8; *t*BuCN, 630-18-2; PhCN, 100-47-0; EtCN, 107-12-0; *n*PrCN, 109-74-0; *n*BuCN, 110-59-8.

(34) Since the nitrile pressure is 5×10^{-7}–2×10^{-6} Torr, a rigorous treatment must also consider that the collisional rate constant for **1** and acetonitrile is ≈4.7 times that for **1** and Kr and 4.3 times that for **1** and Ar. Thus, if the acetonitrile pressure is 1×10^{-6} Torr, Kr pressure = 2×10^{-6} Torr, efficiency = 0.05, $k_c = 2.2 \times 10^{-9}$ cm^3 s^{-1}, and $k_c'[B] = (k_L[Kr] + k_c[CH_3CN])$, then $k_b = 1500$ s^{-1}, where k_L is the Langevin rate constant for **1** and Kr.

(35) Caldwell, G.; Bartmess, J. E. *J. Phys. Chem.* **1981**, *85*, 3571 and references therein.

(36) Samuel, E.; Rausch, M. D. *J. Am. Chem. Soc.* **1973**, *95*, 6263.

(37) Jordan, R. F.; Bradley, P. K.; Baenziger, N. C.; LaPointe, R. E. *J. Am. Chem. Soc.* **1990**, *112*, 1289.